Deciphering the properties of hemp seed oil bodies for food applications: Lipid composition, microstructure, surface properties and physical stability

Christelle Lopez, Bruno Novales, Hanitra Rabesona, Magalie Weber, Thierry Chardot, Marc Anton

Deciphering the properties of hemp seed oil bodies for food applications: lipid composition, microstructure, surface properties and physical stability

Christelle Lopez [1]*, Bruno Novales [1,2], Hanitra Rabesona[1], Magalie Weber [1], Thierry Chardot [3], Marc Anton [1]

[1]INRAE, UR BIA, F-44316, Nantes, France

[2]INRAE, BIBS facility, F-44316, Nantes, France

[3]INRAE, AgroParisTech, Université Paris-Saclay, Institut Jean-Pierre Bourgin, F-78000 Versailles, France

*Corresponding author: Christelle Lopez

Christelle.lopez@inrae.fr

Abstract

Hemp seed oil bodies (HSOBs) are of growing interest in response to the demand of consumers for healthy and natural plant-based food formulations. In this study, we used minimal processing including aqueous extraction by grinding and centrifugation to obtain HSOBs. We determined the lipid composition of HSBOs, their microstructure, and the impact of the homogenization pressure, pH and minerals on their surface properties and the physical stability of the emulsions. HSOBs contain high levels of well-balanced PUFA with LA/ALA=2.9, γ-tocopherol, lutein and phytosterols. The mean diameter of HSOBs was 2.3 ± 0.1 µm with an isoelectric point in the range of pH 4.4 to 4.6. Homogenisation of hemp seed extracts induced a decrease in the size of HSOBs but did not eliminate the sedimentation of the protein bodies composed of the globulin edestin. By changing the surface properties of HSOBs, pH values below 6 and NaCl induced the aggregation of HSOBs, while $CaCl_2$ induced both aggregation and membrane-fusion mediated coalescence of HSOBs by involving probably the anionic phospholipids together to membrane proteins. This study will contribute to extend the range of novel food products and designed emulsions containing hemp seed proteins and OBs.

Keywords: lipid droplet, oil body, interface, membrane, natural oil in water emulsion, homogenization, plant based food source

1. Introduction

Consumers do expect more natural, minimally processed, of high sensorial quality, nutritionally interesting, and healthy food products (Battacchi et al., 2020; Román et al., 2017). The ever-increasing demand of consumers for plant-based diets, including foods containing plant-based proteins of nutritional interest and lipids rich in polyunsaturated fatty acids (PUFA; mainly *n*-3 FA) and other bioactive compounds, is in the spotlight and has made it essential to find and characterize additional sources of plant nutrients. Oilseeds are among the most promising sustainable plant-based

food sources since they contain proteins and lipids in the form of natural oil bodies (OBs; also called lipid droplets, oil droplets or oleosomes), both of which are essential for structuring food systems such as emulsions and emulsion filled gels and for providing nutrients.

In this food transition context promoting sustainable diets, there has been a growing interest in the last decade for hemp (*Cannabis Sativa L.*). Hemp cultivation has a low environmental impact and is adapted to mild climate, whole hemp can be valorized and provides hemp seeds of nutritional interest and health benefits (Farinon et al., 2020; Rupasinghe et al., 2020; Sorrentino, 2021). Hemp seeds typically contain 25-35% lipids with over 80% amount of PUFA and a unique and perfectly balanced essential fatty acid composition, i.e. ratio *n*-6 linoleic acid / *n*-3 α-linolenic acid around 3 as recommended for human nutrition (Simopoulos, 2002). Hemp seeds also contain 20-25% proteins (65-75% of globulin edestin, water-soluble albumins) of high biological value, easy to digest and rich in essential amino acids, 20-30% carbohydrates (with mainly insoluble dietary fibre), as well as vitamins and minerals (Farinon et al., 2020). Hemp seeds are praised for providing adequate quantities of different nutrients to satisfy human dietary requirements (Rupasinghe et al., 2020). Currently, hemp seeds are processed mainly by cold mechanical pressing or with the use of organic solvents such as hexane to maximize the extraction yield of the valuable hemp oil and valorize the hemp proteins by extraction from the cakes and transformation into powdered ingredients (hemp protein concentrates or isolates) (Potin and Saurel, 2020).

Over the last two decades, the scientists and food manufacturers have increased their interest in the natural properties of biological entities of plant origin such as the OBs, which can be recovered along with proteins by aqueous extraction from seeds (Ntone et al., 2020). OBs are lipid-based nature-assembled colloidal structures synthetised by plants to store the energy they need for germination and growth. They are naturally designed to deliver nutrients, mainly the triacylglycerols (TAG), and other biological components of nutritional and heath interests (Acevedo-Fani et al., 2020). OBs could therefore be futher valorized in human diet, for example in complex food systems such as fermented products, in response to the need of consumers to find green, biocompatible and natural

components in their diet. The use of natural OBs was suggested for dressings, sauces, dips, beverages and desserts (Nikiforidis et al., 2014), and plant-based emulsion products such as mayonnaise (Romero-Guzmán et al., 2020). However, the current lack of understanding of the microstructure and surface properties of OBs in response to changes in pH and mineral environment, associated to the physical stability of the emulsion poses a significant barrier to the development of OBs-based new food products.

OBs are naturally emulsified delivery systems for a number of bioactive molecules including PUFA, tocopherols, carotenoids and phytosterols. The structure of mature OBs consists of a central hydrophobic core containing plant TAG (up to 94-98 wt%) and sterol esters. The TAG core is stabilized by a complex interfacial layer consisting of 0.6 – 2 wt% phospholipids and 0.6 – 3 wt% specialized integral membrane proteins such as the oleosins (15-26 kDa), the calcium-binding caleosins (25-35 kDa) and steroleosins (40-60 kDa) (Nikiforidis et al., 2014; Tzen et al., 1993). As the main membrane proteins, oleosins play a key role in the physical stabilization of the OBs against coalescence by electrostatic repulsion and steric effects (Maurer et al., 2013). The interfacial structure of OBs is further reinforced by electrostatic interactions between the positively charged residues of the oleosins and the negatively charged groups of the phospholipids (White et al., 2008). The naturally-occuring interface, mainly composed of membrane proteins and phospholipids, protects the TAG core of OBs from oxidation, rendering the use of antioxidant agents unnecessary (Kapchie et al., 2013).

Oil-in-water emulsions in foods can be exposed to different pH values and mineral stressful conditions (e.g. presence of calcium) that could affect their physical stability through several mechanisms including creaming, flocculation, and coalescence. The applications of natural OBs as functional ingredients are closely related to their physical stability in foods. A fundamental understanding of the physical stability of natural emulsions containing hemp seed OBs, under variable conditions such as pH and ionic strength, would allow their incorporation into selected food systems.

The objectives of this work were to characterize the lipid composition of natural OBs obtained by minimal processing including aqueous extraction from hemp seeds, to examine their microstructure, and to determine the impact of homogenisation, pH and minerals (various NaCl and $CaCl_2$ concentrations) on their surface properties and the physical stability of the emulsions.

2. Materials and methods

2.1. Materials

Whole hemp (*Cannabis sativa L.*) mature seeds from organic agriculture were produced by Nunti-Sanya (Les chanvres de l'Atlantique, Saint Geours de Maremne, France), and purchased from Biocoop (Landivisiau, France). The composition of the hemp seeds as provided by the seed producer was as follows: proteins = 21 g/100 g ; carbohydrates = 7.4 g/100 g ; fibers = 30.6 g/100 g ; lipids = 31.2 g/100 g. The classes of fatty acids (FA) were as follows: saturated FA 3.3 g/100 g, monounsaturated FA 5.6 g/100 g, polyunsaturated FA 22.3 g/100 g with linoleic acid 18:2*n*-6 (LA) 16.3 g/100 g and alpha-linolenic acid 18:3*n*-3(ALA) 5.7 g/100 g and the LA/ALA ratio = 2.9.

Sodium chloride (NaCl) and calcium chloride ($CaCl_2$) were obtained in analytical grade from Sigma-Aldrich (St Louis, MO, USA). D(+)-sucrose was purchased from VWR Chemicals (St Louis, USA). Ultrapure (milliQ) water filtered with a Merck Millipore device (Darmstadt, Germany) was used to perform the aqueous extractions, to recover oil bodies and protein bodies, and to dilute samples where appropriate.

2.2. Samples preparation

2.2.1. Oil body aqueous extraction

Oil bodies were recovered from hemp seeds by applying aqueous extraction associated to a mechanical treatment. Hemp seeds (batches of 100 g) were soaked in ultrapure water (1:3 w/v) for 20h at 20°C to allow their hydration. After soaking, the dispersion of seeds in water was ground for 3 min at a speed of 6000 rpm (Turbomix plus, Moulinex, France) to disrupt the cell walls and release

the cellular material. The resulting slurry was then filtered through a layer of cheesecloth to remove the external part of the seeds (solid residues) and cell wall components. The filtrate corresponded to the hemp seeds aqueous extract, which is called extract in this paper. Hemp seed extract is a natural oil-in-water emulsion that contains OBs and plant storage proteins. In order to isolate OBs, hemp seed extract was centrifuged at 1000 *g* for 30 min at 20°C (Eppendorf® 5810R centrifuge, Merck KGaA, Darmstadt, Germany). The layer of OB-rich cream at the top of the tubes was manually collected. The protein bodies were obtained as sedimented material after centrifugation of the hemp seed extract at 4000 *g* for 30 min.

In an alternative to mechanical grinding, minimal processing was applied to the hydrated hemp seeds: they were cutted with a knife, which induced the release of hemp seed components in the aqueous phase.

2.2.2. Homogenization

The hemp seed extracts were passed through a two-stage laboratory high-pressure homogenizer (PandaPlus 1000, GEA, Italy) at 40°C. Homogenization was performed at 10, 30 and 60 MPa. The hemp seed extracts, without homogenization and after homogenization, were centrifuged at 4000 *g* for 30 min to collect on the top the cream that was rich in natural OBs or homogenized OBs (noted H-OBs) and on the bottom the pellet of sedimented proteins, in order to perform additional characterizations (particle size measurements, confocal microscopy, chemical analysis). The non homogenized and homogenized hemp seed extracts were stored at 4°C in order to characterize their physical stability as a function of time.

2.2.3. Changes in the pH and mineral environment

The pH of OB suspensions was adjusted using 0.1 M HCl or NaOH solutions. Solutions of NaCl and $CaCl_2$ were prepared by dissolving the required amount of the respective powders in ultrapure (milliQ) water and adjusting the pH to 7.2. The OBs obtained by centrifugation were added to the solutions to reach the final concentration of 8 wt% of lipids in the form of OBs. The samples have

been stored at room temperature for 4h and then stored at 4°C to follow their physical stability as a function of time.

2.3. Chemical analysis

2.3.1 Extraction and quantification of total lipids

The lipid content of the whole hemp seeds was determined in triplicate by Soxhlet extraction with petroleum ether as a solvent (Ntone et al., 2020). For the extraction of total lipids from the cream concentrated in hemp seed OBs, the protocol of the cold extraction procedure developed by Folch and collaborators was used (Folch et al., 1957). The quantification of total lipids from the OBs-rich creams was performed in triplicate, from 3 independent experiments (n = 9). The lipid classes were determined by high-performance thin-layer chromatography (HPTLC; CAMAG® HPTLC, Chromacim SAS, Moirans, France) on silica plates (HPTLC Silica gel 60 F254 10x20 cm, 200 µm, Merck) with the mixtures diethyl ether/acetone (80:20, v/v; on 3 cm) and then hexane/diethyl ether/acetic acid (80:20:1, v/v/v), and revealed using copper sulfate (5 min, 100°C).

2.3.2. Fatty acid profile of hemp seed OBs

The fatty acid profile was determined by a gas chromatography (GC) procedure after methylation with cold methanolic solution of potassium hydroxide. The fatty acid methyl esters (FAMEs) were analyzed by GC (Focus GC, Thermo Electron Corporation, Massachusetts, USA) equipped with a split injector (ratio of 1/20), a CPCil 88 Varian capillary column (50 m × 0.25 mm with a 0.2-µm thick film; Chrompack, Middelburg, The Netherlands) and 1 mL/min of helium as carrier gas. FAME were analyzed using a flame ionization detector and ChromCard Data System (version 2005; Thermo Electron Corporation, Massachusetts, USA). The FAME were identified using a mixture of methyl esters as external standard (Mixture ME 100, Larodan, Sweden). The GC analysis was performed in triplicate for each Folch extract of total lipids from hemp seed OBs.

2.3.3. Quantification of total and individual sterols and sterol esters

The identification and quantification of sterol esters was performed after fractionation of the Folch extracts according to (ISO-8420, 2002) to recover the apolar fraction, and then according to (ISO-122228-1, 2014). For the identification and quantification of total sterols, saponification of hemp seed OBs Folch extract was performed with 15% KOH ethanolic solution, during 22 h in the dark at room temperature. Then, deionized water and n-hexane were added and vigorously mixing on a vortex. After separation of phases, the n-hexane fraction was evaporated under nitrogen stream until dryness. The dried unsaponified material was derivatized with 100 µL of silylating agent (Sylon HT Kit) for 2 h in the dark at room temperature. After that, the reagent was evaporated under nitrogen stream and the residue was dissolved in 1.0 mL of n-hexane. The solution was subjected to centrifugation at 5,000 *g* for 5 min, and the upper phase was then transferred into vials suitable for gas chromatography with flame ionization (GC-FID) analysis. A GC-2010 gas chromatograph equipped with a split/splitless injector and a flame ionization detector (Shimadzu, Kyoto, Japan) was used with a capillary silica column DB (60 m x 0.25 mm x 0.25 µm; Varian). The different phytosterols were identified by comparing the retention times with the individual standards (Sigma-Aldrich). The internal standardard 5α-cholestan-3β-ol (Sigma D6128) was employed to quantification, by the ratio between the concentration and peak areas of phytosterols and internal standard.

2.3.4. Quantification of total and individual carotenoids

The identification and quantification of the carotenoids was performed as in (NF-EN-12823-2, 2001). The saponification of hemp seed OBs Folch extract was performed as for sterol analysis. The carotenoids were extracted from the KOH/ methanolic phase and were analysed by HPLC (column C18 Vydac 250 x 4mm) in isocratic conditions and detected at 450 nm. The individual carotenoids were identified by using external standards. For quantification, the external standard beta-carotene (Sigma-Aldrich) was used.

2.3.5. Quantification of total and individual tocopherols and tocotrienols

The quantification of total and individual tocopherols and tocotrienols was performed on Folch extracts according to (ISO 9936:2016). Tocopherols standards (purity > 95%) were provided by Sigma-

Aldrich (St. Louis, MO). HPLC analysis was performed using the 1290 Agilent System (Massy, France) equipped with a C18 column (250 mm × 4.6 mm i.d., 5 µm, HALO(R)-5 column, AMT, Wilmington, Delaware, USA) and a fluorescence detector (296 nm for excitation and 330 nm for emission). The mobile phase consisted of ethanol/methanol (40:60 v/v) in isocratic conditions. The temperature of the column was maintained at 25°C and the flow rate was 0.8 mL/min. Each sample was analyzed in triplicate.

2.3.6. Polar lipid analysis of hemp seed OBs

The quantification of total phospholipids and the determination of the individual phospholipid classes in hemp seed OB samples were performed using HPLC combined with an evaporative light scattering detector as previously described (Lopez et al., 2014). The identification of the phospholipids was carried out by a comparison with the retention time of pure standards. Quantitatification was performed using calibration curves.

2.3.7. Protein quantification

The determination of the protein content was carried out by spectrophotometric measurement using a colored chemical reaction with bicinchoninique acid (BCA) according to Smith et al. (1985). BCA Assay kit were from Uptima Interchim (Montluçon, France). Briefly, 25 µl of each sample were loaded on microplate in triplicate and 200 µl of a mix of Reagent A and B was added. Bovin Serum Albumin (BSA ; 2 mg/mL) with different dilutions (0 µg to 1000 µg) was used for calibration curve. After incubation at 37°C for 30 min, the reading of the microplate was performed at 562 nm on microplate spectrophotometer (Epoch, BioteK Instruments, France). Concentration of proteins was determined after calculation from BSA standard curve taking into account the dilution factors of each sample.

2.3.8. Gel electrophoresis

2.3.8.1 Preparation of the samples before gel electrophoresis

The hemp seed extracts, without homogenization and after homogenization at 10, 30 and 60 MPa, were centrifuged at 4000*g* for 30 min to recover the cream (top), the intermediate supernatant aqueous phase and the sedimented centrifugation pellet (bottom).

For the determination of the interfacial protein composition of native OBs or homogenized OBs (H-OBs) by gel electrophoresis, OBs and H-OBs were isolated from the aqueous phase to remove un-adsorbed proteins from the interface according to a method adapted from Patton and Huston (1986). Briefly, 10 g of the creams were mixed with 10 g of a solution containing containing 50% w/w of sucrose. Then, in 50 mL plastic centrifuge tubes, 20 g of the treated hemp seed extract were delivered under 30 g of a solution containing 5% w/w of sucrose. The tubes were centrifuged at 4000*g* for 30 min in order to form a layer of washed OBs or H-OBs at the top of the tubes.

2.3.8.2 Gel electrophoresis

The proteins contained in all the samples used for gel electrophoresis were quantified by BCA Assay and the protein composition was characterized by SDS-PAGE with Mini-Protean TGX Precast Gels 12% using Mini-Protean Tetra Cell system (Bio-Rad Life Science, France). All reagents are from Bio-Rad Life Science. The different protein samples were diluted in denaturing and reducing buffer. Samples were diluted in 2x Laemmli sample buffer in reducing conditions with 2-mercaptoethanol 5% (a reducing agent that breaks down the disulfide linkages). The migration buffer contained 25 mM Tris, 192 mM glycine, 0.1% SDS according to Laemmli (1970) protocol. The samples were heated at 100°C for 5 min. Each protein sample was then loaded on a sample well (20 µg of protein/well) of the 12% polyacrylamide gel electrophoresis. Molecular weight (MW) protein markers from MW 3 to 198 kDa (SeeBlue Pre-stained Protein Standard, Novex Thermo Scientific, Les Ulis, France) and from MW 14.4 to 116 kDa (unstained Molecular weight marker, Euromedex, Souffelweyersheim, France) were used for MW calibration. The migration was carried out at 150 V for 45 min. The gel was stained with Coomassie Brilliant Blue G-250 staining solution for 2h with gentle agitation on platform rocker according to Lawrence and Besir (2009). The gel was rinsed with distilled water before scanning on a flatbed scanner (Image Scanner iii, GE Healthcare, Souffelweyersheim, France).

2.4. Physico-chemical characterisations

2.4.1. Particle size measurements

The size distributions of OBs and protein bodies (PBs) were determined by using a laser diffraction analyzer (Horiba LA-960V2, Retsch Technology, Germany). The refractive indexes used were 1.47 for the OBs, 1.45 for the proteins, and 1.33 for the continuous phase (water). For measurements, the samples were diluted as appropriate in ultrapure water. The particle size measurements of each sample were performed at room temperature and in triplicate using three different samples.

2.4.2. Zeta potential measurements

Dispersions of OBs were diluted in solutions of various pHs or containing various amounts of NaCl or $CaCl_2$ (100 µl OB dispersion in 10 mL solution). Diluted OB dispersions were filled into a cuvette, which was then placed into the chamber of a Zetasizer Nano ZS (Malvern, Germany). The zeta potential was calculated from the electrophoretic mobility of the OBs according to the Smoluchowski approximation and Henry's law. The measurements were run five times at 25°C on at least three independent and freshly prepared samples.

2.5. Microstructure

The microstructures of hemp seed extracts and OBs were examined by confocal laser scanning microscopy (CLSM) using a microscope NIKON A1R (NIKON, Champigny sur Marne, France) with a x60 oil immersion objective. The lipid-soluble Nile Red fluorescent probe (5H-benzo-alpha-phenoxazine-5-one,9-diethylamino; supplied by Sigma Aldrich, St Louis, USA; 100 µg/mL in propanediol) was used to stain the TAG (excitation wavelength = 560 nm). Fast Green FCF (Sigma-Aldrich, St. Louis, USA ; 10 mg/mL in water) was used to stain proteins (excitation wavelength = 636 nm). The fluorescent head group-labelled phospholipid analogue Lissamine rhodamine B sulfonyl dioleoylphosphatidylethanolamine (Rh-DOPE, 1 mg/mL; Avanti Polar lipids Inc., Birmingham, England) was used to characterize the hydrated hemp seeds and to investigate the lateral distribution of phospholipids on the surface of OBs (excitation wavelength = 560 nm). The samples were kept at room temperature for at least 30 min prior to observation by CLSM.

3. Results and discussion

3.1. Lipid composition of hemp seed OBs

The hemp seeds used in this study contained 33.6 ± 0.5 g of total lipids / 100 g of seeds, which was in accordance with information given by the seed producer and with data found in literature (Farinon et al., 2020). The lipid composition of the hemp seed OBs obained by aqueous extraction and centrifugation is presented in **Figures 1 and 2**. The schematic representation of a hemp seed OB proposed **Figure 1-A** illustrates the localisation of the main components. As expected, lipid class analyses confirmed the main amount of triacylglycerols (TAG ~ 95% of lipids; **Fig 1-B**), and the presence of diacylglycerols, free fatty acids, phytosterols, tocopherols, carotenoids, and phospholipids in hemp seed OBs. The fatty acid (FA) profile of hemp seed OBs showed that linoleic acid (C18:2 *n*-6 ; LA), α-linolenic acid (C18:3 *n*-3 ; ALA) and oleic acid (C18:1 *n*-9) were the most abundant FAs which together comprised 84.1% of the total FAs (**Fig 1-C**). The PUFAs of the oil amounted to 72.9% of the total of FAs while the monounsaturated and saturated FAs amounted to 13.6 wt% and 9.2 wt%, respectively. The hemp seed OBs deliver the essential PUFAs *n*-6 and *n*-3 in the proportion 3:1 that is the best ratio recommended by medical research and the most advanced theories in the field of nutrition. Our results on the FA composition of hemp seed OBs were in agreement with literature on hemp seeds and oil (Farinon et al., 2020; Montserrat-de la Paz et al., 2014).

Hemp seed OBs contained 206 ± 7 mg phospholipids / 100 g lipids (0.21 wt%). The relative proportion of the individual OBs phospholipids is presented **Figure 1-D**. The main phospholipids of hemp seed OBs were the zwitterionic phosphatidylcholine species (PC ; 32.3 wt% PL), in agreement with literature (Antonelli et al., 2020). The zwitterionic phosphatidylethanolamine (PE) accounted for 11.3%wt of total phospholipids. The anionic phospholipids phosphatidylserine (PS ; 10.1 wt% PL) and phosphatidylinositol (PI ; 12.5 wt% PL) were also detected, in agreement with literature (Furse et al.,

2013; Tzen et al., 1993). Phosphatidic acid (PA) accounted for 30.4 wt% PL. Altogether, the anionic phospholipids (sum of PS, PI and PA) accounted for 53 wt% of total phospholipids.

The unsaponifiable fraction of hemp seed OBs contained carotenoids (**Fig 2-A**), tocopherols (**Fig 2-B**) and phytosterols (**Fig 2-C**). The carotenoids accounted for 8.3 $\pm$ 0.3 mg/100 g lipids (2.8 mg/100 g hemp seeds), with the three main carotenoids being lutein (80 wt% carotenoids ; 6.6 $\pm$ 0.2 mg/100 g lipids; 2.2 mg/100 g hemp seeds), beta-carotene and zeaxanthin, in agreement with literature (Farinon et al., 2020). The sum of tocopherols and tocotrienols accounted for 84.4 $\pm$ 0.8 mg / 100 g of lipids. The tocopherol profile revealed that γ-tocopherol was the most abundant isomer, i.e. 96.7 wt% of total tocopherols, in agreement with literature on hemp (Farinon et al., 2020; Montserrat-de la Paz et al., 2014). Natural fat-soluble functional compounds with high antioxidative activity such as the tocopherols are therefore intrinsically associated to hemp seed OBs. The phytosterol amount was 341.5 $\pm$ 3.6 mg / 100 g of lipids. The main phytosterols characterised in hemp seed OBs were β-sitosterol (67 wt% sterols; 228 mg/100 g of lipids), campesterol, δ5-avenasterol and stigmasterol, which is in agreement with literature (Farinon et al., 2020; Montserrat-de la Paz et al., 2014). The sterols in the esterified form corresponded to about 50 wt% of total sterols (**Fig. 2-C**).

3.2. Microstructure

Figure 3 shows the microstructure of hydrated hemp seeds, hemp seed extracts and OBs. At the microscopic level, and according to their size, mainly the OBs and the PBs were observed. Within the hydrated hemp seeds, the OBs and the PBs appeared closely packed with OBs filling the space between PBs. Both the OBs and the PBs exhibited a spherical shape, with a larger size observed for PBs compared to OBs (**Fig 3-A**), in agreement with observations of peanut seeds and soybean cotyledon (Nikiforidis et al., 2014; Zaaboul et al., 2018). The specific labelling of phospholipids revealed their localisation in membranes within the seed and around the OBs (**Fig 3-A3**).

The mechanical processes applied to the hydrated seeds induced the release of individual OBs and PBs, both of spherical shape, as well as other soluble components and their homogeneous dispersion

in the aqueous extract. Hemp seed extract is therefore a natural oil-in-water emulsion and a dispersion of proteins (**Fig 3-B**). The size distributions of the hemp seed OBs and PBs determined by laser light scattering were monomodal and ranged from 0.3 to 8 µm for OBs and from 1.3 to 20 µm for PBs (**Fig 3**-**B**). The volume-averaged diameters of hemp seed OBs and PBs were 2.3 ± 0.1 µm and 4.1 ± 0.3 µm, respectively. This is in accordance with the size of OBs reported in literature. The volume-averaged diameters of sesame and peanut OBs were reported to be 2.4 ± 0.4 µm and 2.3 ± 0.3 µm respectively, with sizes ranging from 1 to 10 µm (Yang et al., 2020). The similar OB sizes observed by CLSM inside the seeds (**Fig 3-A**) and after the aqueous extraction by grinding (**Fig 3-B**) indicated that the hemp seed OBs have not been mechanically disrupted during preparation.

The hemp seed OBs showed a large core region rich in TAG (**Fig 3-C**). CLSM images of hemp seed OBs revealed non-fluorecent areas in the core of OBs. They were located at the periphery of OBs and absent from the internal core of the OBs, as revealed by observations at different z-depths (**Fig 3-C1**). According to previous observations reported in literature (Czabany et al., 2008), the structures revealed by CLSM could correspond to steryl esters in an ordered state that segregated from the fluid TAG phase.

CLSM observations showed a heterogeneous distribution of proteins at the surface of hemp seed OBs (**Fig 3-C**). These proteins located at the surface of native OBs could correspond to the specific membrane-associated proteins described for OBs (oleosins, caleosins and steroleosin; **Fig. 1-A**) (Nikiforidis et al., 2014; Tzen et al., 1993).

The monolayer of phospholipids on the OB surface, that delimit their hydrophobic TAG core, was investigated (**Fig 3-D**) and revealed areas in which the Rh-DOPE fluorescent dye was not able to integrate (**Fig 3-D3**). These areas could correspond to the concentration of proteins embeded in the fluid matrix of phospholipids (i.e. oleosins, caleosins and steroleosin) or to ordered domains formed for example by sterols in the plane of the phospholipid monolayer. The heterogeneous distributions of proteins and phospholipids at the surface of hemp seed OBs that have been observed in this study

contrast with the uniform layers of proteins and phospholipids reported on the surface of OBs from almond milk and coconut milk (Dave et al., 2019; Gallier et al., 2012).

3.3. Homogenization to improve the physical stability of hemp seed extracts

The physical stability of hemp seed extracts as a function of time and the impact of high-pressure homogenization were investigated (**Figures 4 and 5**). Freshly prepared hemp seed extracts showed spontaneous phase separation within a few hours with partitioning into a sedimented layer, a milk-white phase and a top cream layer (**Fig. 4-C**). A technological process able to decrease the size of the particles and avoid phase separation upon long-time storage is high-pressure homogenization. Hemp seed extracts were therefore submitted to homogenization under various pressures ranging from 0 to 60 MPa. CLSM observations of the hemp seed extracts showed the coexistence of OBs with a decrease in their size as a function of the increase in the homogenization pressure, and large spherical PBs (**Fig 4-A**). Some OBs were in interaction with PBs after homogenization (**Fig 4-A, insert**). The size distributions of the non-homogenized and homogenized hemp seed extracts, as well as the size distributions of the OBs and PBs that have been selectively separated from the homogenized samples by centrifugation, are presented **Figure 4-B**. High-pressure homogenization successfully decreased the diameter of hemp seed OBs while it induced a small reduction in the diameter of the PBs (**Fig. 4-B5**). The mean diameter of OBs decreased from 2.3 µm (size range: 0.3 to 8 µm) to 0.26 µm (size range: 0.08 to 0.8 µm) after homogenization at 60 MPa. The mean diameter of PBs decreased from 4 µm (size range: 1.3 to 20 µm) to 2.6 µm (size range: 0.9 to 6 µm; 60 MPa).

Further chemical and microscopic observations were performed in order to identify the components in the sedimented material and in the top cream layer (**Fig. 5**). Gel electrophoresis showed that the globulin edestin, including its acidic sub-units (33 kDa) and basic sub-units (20 kDa), was the major protein of the hemp seed extracts in accordance with litterature (Malomo et al., 2014; Tang et al., 2006). The protein 7S globulin (48 kDa) and the water-soluble albumins (below 20 kDa) were also detected. The sedimented material (pellet after centrifugation) was mainly composed of edestin

while the supernatant contained water-soluble proteins. Similar results were obtained for unhomogenized and homogenized hemp seed extracts (**Fig. 5-A**). The globulin edestin was recovered in the sedimented material as a consequence of its higher density than the density of water (density of PBs from seeds around 1.3 ; (Tully and Beevers, 1976)) and low solubility in water since edestin is a salt-soluble globulin. Indeed, the globulin edestin requires high ionic strength solvents to be solubilised, for example sodium phosphate/sodium chloride buffer at pH 7.8 with a ionic strength of 500 mM (St Angelo et al., 1968). The top cream layer was rich in OBs, as a result of their low density in comparison to water. The proteins adsorbed at the surface of natural and homogenized OBs were identified. As expected (**Fig. 1-A**), oleosins isoforms (15 – 20 kDa), caleosin (35 kDa) and steroleosin (50 kDa) were identified as interfacial proteins of the natural OBs (**Fig. 5-A**). Increasing the homogenization pressure induced changes in the interfacial protein composition of the H-OBs, with an increased relative proportion of edestin, as shown by the presence of its acidic sub-units (33 kDa) and basic sub-units (20 kDa). These results showed that the increase in the OBs surface area associated to the decrease in their size as a function of the homogenization pressure applied induced the adsorption of edestin to stabilize the interface created upon homogenization. Interestingly, gel electrophoresis showed the presence of oleosin isoforms at the surface of H-OBs even after homogenization at 60 MPa (**Fig. 5-A**).

CLSM observations showed that, in absence of homogenization, the top layer formed as a function of time or obtained after centrifugation was enriched in natural OBs of larger size than in the supernatant while the sedimented material or pellet obtained after centrifugation corresponded mainly to PBs characterized by their spherical shape, e.g hemp seed's globulin edestin (**Fig. 5-B**). In the samples homogenized at 10 MPa, the sedimented material was composed of PBs alone, and of complexes formed between PBs and OBs of small size induced by homogenization as shown by CLSM (**Fig. 5-B6**). The density of the PBs-OBs complexes depends on the relative proportion of lipids and proteins (such as for lipoproteins). The large size, low solubility in water and high density of the hemp seed PBs associated with the small size and low density of the H-OBs induced the

sedimentation of the PBs-OBs complexes. In the samples homogenized at 10 MPa, the top cream layer contained small particles of proteins in interaction with the homogenized OBs, as shown in **Fig. 5-B4**. The adsorption of water-insoluble particles of hemp seed proteins, mainly the colloidal PBs composed of edestin, at the surface of homogenized OBs opens perspectives for their potential utilization as stabilizers in food-grade Pickering emulsions (Sarkar and Dickinson, 2020).

As a conclusion, the homogenization process induced a physical stabilization of the hemp seed OBs for homogenization pressures above 10 MPa by reducing their size below 1 µm (**Fig. 4-B**) but the large PBs sedimented as a consequence of their size larger than 1 µm, their poor water solubility and their high density (**Fig 4-C; Fig. 5**). The impact of high-pressure homogenization that affects both the composition and the architecture of the natural OBs surface, on the oxidative alteration of OBs PUFA will be further investigated by our group.

3.4. Impact of pH and minerals on the surface properties of OBs and physical stability of the emulsions

3.4.1. Impact of pH

The ζ-potential values of hemp seed OBs, obtained either by minimal mechanical processing or by mechanical grinding of the hydrated hemp seeds, were determined as a function of pH (**Fig 6**). The mechanical treatments used during aqueous extraction of the hemp seed OBs did not significantly affect the ζ-potential values measured as a function of pH, indicating an absence of changes or alteration of the surface properties of the OBs. The ζ-potential of the OBs decreased from negative to positive with decreasing pH (**Fig 6-A**). Above pH ≥ 9, the ζ-potentials of the OBs reached a plateau with ζ = -55 mV. The absolute values of ζ-potential measured for hemp seed OBs decreased with pH until reaching the isoelectric point (IEP ; ζ = 0 mV) in the range pH 4.4 - 4.6 (**Fig 6-A**). For pHs below the IEP, the ζ-potential values were positive, with ζ = +40 mV below pH3. This is in agreement with previous studies reporting that the ζ-potential of maize OBs ranged from -40 mV at pH 7 to +35 mV at

pH 3 (Nikiforidis and Kiosseoglou, 2009). The ζ-potentials of sesame OBs, peanut OBs, sunflower OBs and soybean OBs have been reported to follow similar trends ranging from -25 to -35 mV at pH 8 to +25 mV at pH 2 (Wang et al., 2019; Yang et al., 2020). The IEP found in this study for hemp seed OBs is in agreement with the zero charge point reported between pH 4.5 and pH 5 for maize OBs (Nikiforidis and Kiosseoglou, 2009), as well as for sesame, soybean, sunflower and peanut OBs (Qi et al., 2017; Wang et al., 2019; Yang et al., 2020).

The physical stability of the emulsions containing hemp seed OBs was examined as a function of pH and combined with structural observations performed by confocal microscopy (**Fig 6 B & C**). Changes in pH affected the physical stability of the hemp seed OBs. For pH values above pH 7.5, the OBs in water emulsions were physically stable, in accordance with strong electrostatic repulsions due to the negative charge of the OBs at this pH (-30 to -55 mV ; **Fig. 6-A**). For $3.3 \leq pH \leq 7.1$, a layer concentrated in OBs was rapidly formed at the top of the samples (**Fig. 6-B)**. The bottom of the samples was turbid from pH 5.5 up to pH 7.1 while it was clear for $3.3 \leq pH \leq 5.8$. In this range of pHs, CLSM observations revealed the formation of OBs aggregates (**Fig. 6-C**). At pH 6.2, small OBs aggregates were observed. The sizes of the OBs aggregates were larger below pH 6. CLSM images showed that the proteins corresponding mainly to oleosins located at the surface of OBs were involved in the formation of the OBs aggregates. For pHs ranging from to 5.0 to 4.5, that correspond to the IEP of hemp seed OBs (**Fig. 6-A**), large aggregates of OBs connected by proteins were observed together with the formation of large OBs formed by coalescence. For pH 3.7 and 3.3, large particles containing aggregated proteins originating from OBs surface and non-spherical oil droplets coalescing at their periphery were oberved (**Fig 6-C**). For pH 2.9, the whole content of the tube was turbid and the samples did not show phase separation at the macroscopic level (**Fig 6-B**), while CLSM observations showed the formation of small aggregates of OBs (**Fig 6-C**).

Our results on the impact of pH are in agreement with previous reports on OBs from other plant sources. Extensive aggregation of sunflower-seed OBs was reported between pH 5 and 6 (around the

455 IEP), without coalescence, and associated to a high creaming (White et al., 2008). OBs isolated from
456 maize maintained their entities at pH 7.2 but aggregated when the pH was lowered to 6.8 and 6.2
457 (Tzen et al., 1992).
458 The composition and structure of the hemp seed OBs surface governed their sensitivity to pH and the
459 physical stability of the emulsion. The overall electronegative charge of hemp seed OBs surface at
460 neutral pH results from i) the presence of charged phospholipids (anionic and containing a negatively
461 charged phosphate group such as PA or within neutral phospholipids such as PC; **Fig 1**), and ii) the
462 topology of the oleosins (main OB-associated proteins) in the OB membrane that expose their
463 negatively charged residues (i.e. the acidic amino acids in the N- and C-termini) to the aqueous phase
464 (Huang, 1994). These negative charges of OBs were reponsible for electrostatic repulsions and
465 physical stability of the OBs-in-water emulsions towards aggregation. Decreasing the pH, i.e.
466 increasing the amount of protons H^+ in the aqueous phase surrounding the OBs, decreased the
467 electrostatic repulsions between OBs. The overall charge of the OBs was insufficient to generate
468 repulsive forces greater than the attractive interactions, hydrophobic and Van der Waals, that were
469 present between the OBs, resulting in OBs aggregation. OBs aggregates of large size phase separated
470 from the aqueous phase and reached the top of the samples due to the low density of oil. Authors
471 reported that the IEP of intrinsic oleosin proteins associated with the surface of the OBs is comprised
472 between pH 5 and 6 (White et al., 2008). When the pH of OBs in water emulsion was close to the IEP
473 of these stabilizing proteins, OBs aggregation occured. The low amount of coalescence of OBs for pH
474 above IEP has been attributed to steric hindrance (Tzen and Huang, 1992; Tzen et al., 1992), but also
475 to the strength of the natural emulsifying layer of OBs due to the association between the N- and C-
476 termini of the oleosin protein with the phospholipids preventing closely associated OBs from losing
477 their integrity (White et al., 2008). The pKa of the charged groups of the phospholipids should also be
478 considered to explain the impact of pH on the hemp seed OBs. The COOH group of the anionic
479 phospholipid PS exhibits a pKa close to 5.5 and the pKa of the phosphate group of the phospholipids
480 is close to pH 3 (Marsh, 2013), which means that the negative charge no longer exist below these key

pH values. Changes in pH affected the individual molecules present at the surface of OBs (phospholipids and proteins) but also possibly the proteins - phospholipids interactions and the conformation of the proteins in the OB hemi-membrane (changes in the exposure of protein hydrophobic regions to the aqueous phase) (Qi et al., 2017).

The impact of pH on the physical stability of hemp seed OBs that leads to aggregation and coalescence should be considered in the formulation of foods, for exemple acidic products such as fermented products and mayonnaise.

3.4.2. Impact of NaCl and $CaCl_2$

The impact of monovalent (Na^+) and divalent (Ca^{2+}) ions on the negatively charged surface of hemp seed OBs was examined at pH 7.2. These cations were provided by NaCl and $CaCl_2$, respectively.

In a first set of experiments, hemp seed OBs were dispersed in presence of various amounts of NaCl, with concentrations varying from 0 to 500 mM (8 wt% OBs in the samples) (**Fig 7**). Changes in the ζ-potential values as a function of the concentration in NaCl are presented **Figure 7-A**. The ζ-potential of OBs decreased quite linearly from ζ = -29.8 $\pm$ 2.2 mV in absence of NaCl to ζ = -9.8 $\pm$ 1.1 mV in presence of 50 mM NaCl, and decreased to a lesser extend for high contentrations in NaCl (ζ = -2.8 $\pm$2.4 mV for 500 mM NaCl). Macroscopic observations revealed a physical instability of the hemp seed OBs induced by NaCl, with the formation of a OB-rich cream layer at the surface of the tubes mainly for concentrations ranging from 20 to 100 mM NaCl (**Fig 7-B**). This was related to the aggregation of hemp seed OBs in presence of NaCl induced by the decrease in the electrostatic repulsions as a result a low zeta potential values. The thickness of the OB-rich cream layer was smaller for NaCl amounts of 200 and 500 mM compared to the range 20 to 100 mM NaCl. This could be attributed to structural reorganisations of interfacial proteins in presence of high amount of NaCl, with steric repulsions between hemp seed OBs. Below the OB-rich cream layer, the turbidity of the samples was high whatever the amount of NaCl, indicating a high proportion of OBs dispersed in the volume. CLSM observations of the samples showed the formation of OB aggregates in presence of

NaCl, with a connectivity between the surface layer of several OBs (**Fig 7-C**). In this study, we showed that NaCl affects the surface properties of OBs components, probably both phospholipids and proteins, with a decrease in ζ-potential values leading to a reduction of repulsive interactions and then to an aggregation of OBs. Large OBs aggregates raised at the surface of the samples and formed the OB-rich cream layer. From the CLSM images, we concluded that NaCl did not induce coalescence of the hemp seed OBs. Our results are in agreement with authors who reported aggregation of OBs from maize at pH 7.2 in presence of NaCl (10 – 1000 mM ; -5 to -20% turbidity) (Tzen et al., 1992).

In a second set of experiments, hemp seed OBs were dispersed in presence of various amounts of $CaCl_2$, with concentrations ranging from 0 to 10 mM (8 wt% OBs in the samples ; **Fig 8**). Changes in the ζ-potential values as a function of the concentration in $CaCl_2$ are presented **Figure 8-A**. The ζ-potential values decreased from ζ = -29.7 $\pm$ 2.7 mV in absence of $CaCl_2$ to ζ = -5.6 $\pm$ 0.5 mV in presence of 2 mM $CaCl_2$, and to ζ = -0.8 $\pm$ 0.2 mV in presence of 10 mM $CaCl_2$. At pH 7.2, e.g. above the IEP of the OBs, the divalent cations Ca^{2+} were the main counter-ions. They were therefore involved in the reduction of the ζ-potential values measured as a function of the increase in $CaCl_2$ concentration in the OB dispersions. These experiments showed the ability of Ca^{2+} ions to associate with the negatively charged OBs surface composed of membrane-associated proteins and phospholipids (**Fig. 1-A**). At the macroscopic level, the physical instability of the hemp seed OBs leading to creaming was induced by low concentration in $CaCl_2$ (**Fig 8-B**). A OB-rich cream layer was rapidly observed in presence of [$CaCl_2$] $\geq$ 0.4 mM, which corresponded to ζ-potential values below -10 mV. For [$CaCl_2$] $\geq$ 2 mM, the turbidity of the samples below the OB-rich cream layer was low, indicating that most of the hemp seed OBs were concentrated in the cream layer. CLSM observations revealed the formation of OB aggregates in presence of 0.2 mM $CaCl_2$ and above. For [$CaCl_2$] $\geq$ 4 mM, non-spherical and large lipid particles were observed within the OB aggregates. This was interpreted as coalescence of hemp seed OBs (**Fig 8-C**). The impact of $CaCl_2$ on OBs aggregation found in our study is in agreement with previous studies performed by other groups on other sources of OBs. An aggregation of maize OBs was reported at pH 7.2 in presence of $CaCl_2$ above 1 mM (Tzen et al.,

1992), an aggregation of sunflower-seed OBs (emulsion, 10 wt%) was reported at pH 7 in presence of $CaCl_2$ above 5 mM associated with an intensive creaming (White et al., 2008). Despite agregation of OBs has already been reported by several authors, the coalescence of OBs due to the presence of calcium ions has not yet been described.

At neutral pH, cations such as H^+, Na^+ and Ca^{2+} can interact with the negatively charged membrane-associated proteins, and with the negative charge of phospholipids (anionic PS and PI ; phosphate group of PC, PE and PA) present at the surface of hemp seed OBs (**Fig 1-A**). Our experiments showed that the divalent cations Ca^{2+} interacted more strongly with the OB membrane components and had a more important impact on the emulsion physical stability than the monovalent cations Na^+ (**Figure 7 & 8**). This is in agreement with Tzen's group who reported that aggregation of OBs from maize could be induced with 2 mM $CaCl_2$ at pH 7.2, but not with NaCl suggesting that aggregation was due to the association of divalent cations with the negatively charged OB surface (Tzen et al., 1992). The divalent ions are more effective at screening electrostatic interactions and at binding to oppositely charged groups (Israelachvili, 2011), leading to aggregation. Several molecular mechanisms, alone or in combination, could underly the impact of low concentrations in Ca^{2+} ions on the surface properties of OBs. First, Ca^{2+} ions could interact with the negative charges of the membrane-associated proteins exposed to the aqueous phase, and affect the conformation of these proteins with consequences on the surface hydrophobicity leading to OB aggregation. Specifically, Ca^{2+} could interact with the calcium-binding caleosins tightly associated with OBs and may be involved in processes such as OB aggregation and OB membrane fusion as previously reported by others (Naested et al., 2000; Purkrtova et al., 2008). Caleosins on one OB surface may form Ca^{2+}-mediated associations with caleosins located on an other OB surface, which would contribute in OB aggregation and membrane fusion (Naested et al., 2000). Second, Ca^{2+} ions could affect the interactions between the negatively charged phospholipids and the positively charged residues of the membrane-associated proteins located at the surface of OBs. Third, Ca^{2+} ions could interact with the phospholipids through 3 binding

559 sites, i.e. the carboxylate groups (PS), phosphates (PS, PI, PC, PE, PA) and the carbonyl oxygen groups
560 of the phospholipid chains (Melcrová et al., 2016). The scientific literature describes the specific role
561 of Ca^{2+} ions in membrane fusion phenomena and particularly of membranes containing the anionic
562 polar head group PS, through the ability to form an anhydrous $Ca^{2+}(PS)_2$ complex between apposed
563 phospholipid layers during initial aggregation (Wilschut et al., 1981). The fusion, that is defined as the
564 joining of two closely opposed lipid layers to form a single layer, involves the functional role of
565 specific lipids such as PS among the complex composition of natural membranes. The aggregation
566 and the subsequent coalescence of OBs could therefore involve OBs membrane fusion through the
567 action of Ca^{2+} ions on the anionic PS molecules located in the surface monolayer and that represent
568 10 ± 2 wt% of hemp seed OBs phospholipids as determined in our study (**Fig 1**). Deciphering the
569 Ca^{2+}-mediated mechanisms involved in OB membrane fusion would deserve to be further
570 investigated at the molecular level.
571

572 ## 4. Conclusions

573 In this study, we successfully used minimal processing including aqueous extraction by grinding to
574 obtain aqueous dispersions containing hemp seed OBs and PBs. Chemical analyses showed that the
575 nutrient and bioactive compounds of hemp seed OBs, such as PUFA with an optimal n-6/n-3 ratio of
576 2.9, phospholipids, carotenoids with 80 wt% lutein, phytosterols with 67 wt% β-sitosterol, and γ-
577 tocopherols contribute to their nutritional interest and potentiel health benefits and encourage the
578 increased valorization of hemp seed OBs based food products in the human diet. We showed that
579 the size of natural hemp seed OBs and their naturally-occuring surface govern their physical stability.
580 Homogenization of hemp seed aqueous extracts was able to avoid phase separation of OBs for a long
581 time storage by reducing their size, but weakly reduced the size of the PBs that sedimented alone or
582 in interaction with homogenized OBs. We showed that stressful environmental conditions induced by
583 pH and minerals (NaCl and $CaCl_2$) to which they were exposed induced the physical unstability of
584 both the OBs and the emulsions. The results found in this study increased knowledge about the

chemical composition, surface properties and physical unstability of hemp seed OBs due to their size and their ionic environment. This study will undoubtedly contribute in the economic valorization of hemp seed OBs, in extending the range of novel food products containing hemp seed OBs and opens perspectives for the development of hemp seed based emulsions.

Acknowledgements

Christelle Lopez thanks all the UR BIA's members involved in the "hemp project" for stimulating discussions. The authors warmly thank Alain Riaublanc and Adeline Boire (INRAE, BIA, ISD, Nantes, France) for interesting discussions about hemp seed proteins and protein bodies. Valérie Beaumal and Elisabeth David-Briand (INRAE, BIA, ISD, Nantes, France) are acknowledged for help in particle size and zeta potential measurements. Yann Gohon (Institut Jean-Pierre Bourgin, Versailles, France) is acknowledged for interesting discussions about the partitioning of TAGs and steryl esters within the core of oil bodies. Iterg (Canejan, France) is acknowledged for pertinent discussions about lipid analyses.

Declaration of competing interest

The authors declare no conflict of interest.

CRediT authorship contribution statement

Christelle Lopez: Conceptualization, Supervision, Investigation, Writing – original draft and revision.

Bruno Novales: Conceptualization, Writing – original draft and revision.

Hanitra Rabesona: Conceptualization, Investigation, Writing.

Magalie Weber: Conceptualization, Writing – original draft and revision.

Thierry Chardot: Conceptualization, Writing – original draft and revision.

Marc Anton: Conceptualization, Writing – original draft and revision.

Figure caption

Figure 1: Lipid composition of hemp seed oil bodies. **(A)** Schematic representation of a hemp seed oil body ; **(B)** Lipid classes ; **(C)** Fatty acids ; **(D)** Phospholipids. The chemical structures of the main components are indicated in the figures. Abreviations : MAG: monoacylglycerols, DAG: diacylglycerols, TAG: triacylglycerols, FFA: free fatty acids, PL: phospholipids, PC : phosphatidylcholine, LPC : lysophosphatidylcholine, PE : phosphatidylethanolamine, PA : phosphatidic acid, PI : phosphatidylinositol, PS : phosphatidylserine.

Figure 2: Lipid composition of hemp seed oil bodies. **(A)** Carotenoids ; **(B)** Tocopherols and tocotrienols, **(C)** Sterols, including total sterols and sterol esters.

Figure 3: Microstructure characterized by confocal laser scanning microscopy (CLSM). **(A)** Hemp seeds containing protein bodies (PBs : green colour, fast green fluorescent dye) and oil bodies (OBs : Red colour, nile red fluorescent dye in A1 and A2, rhodamine-DOPE fluorescent dye in A3) , **(B)** Dispersion of OBs and PBs obtained by aqueous extraction from hemp seeds observed by CLSM (OBs : Red colour, nile red fluorescent dye ; PBs : green colour, fast green fluorescent dye) and size distributions characterized by laser light scattering; **(C)** Hemp seed OBs with the labelling of their core rich in triacylglycerols (Red colour : nile red fluorescent dye) and membrane-associated proteins (green colour : fast green fluorescent dye) ; **(D)** Hemp seed OBs with the labelling of their monolayer of phospholipids (red colour : rhodamine-DOPE fluorescent dye) and PBs (green colour, fast green fluorescent dye).

Figure 4: Impact of high-pressure homogenization on hemp seed extracts : **(A)** microstructure of hemp seed extracts as a function of the homogenization pressure applied with the labelling of the oil bodies (OBs : Red colour, nile red fluorescent dye) and the protein bodies (PBs : green colour, fast

637 green fluorescent dye) ; **(B)** Size distributions measured by laser light scattering; **(C)** physical stability
638 of hemp seed extracts as a function of the homogenization pressure applied.
639
640 **Figure 5:** Impact of high-pressure homogenization on hemp seed extracts : **(A) Left:** gel
641 electrophoresis showing the protein composition in the hemp seed extract (HSE), and in the
642 supernatant (Sup) and pellets obtained after centrifugation. The results are shown without
643 homogenization and after homogenization with the pressures indicated in the figure. **Right:** gel
644 electrophoresis showing the interfacial protein composition of natural OBs and homogenized OBs,
645 and the protein composition in the HSE without homogenization or after homogenization at 60 MPa.
646 **(B)** confocal laser scanning microscopy images showing the oil bodies (OBs : Red colour, nile red
647 fluorescent dye) and the protein bodies (PBs : green colour, fast green fluorescent dye) in the top
648 cream layer, the supernatant and the pellet obtained after centrifugation as indicated in the figure.
649
650 **Figure 6:** Impact of pH on hemp seed oil bodies (OBs) dispersions obtained by aqueous extraction.
651 **(A)** Zeta-potential of the OBs as a function of pH. The OBs were obtained either by grinding or by
652 minimal processing as indicated in the figure; **(B)** physical instability of OB dispersions as a function of
653 pH ; **(C)** confocal laser scanning microscopy images of OB dispersions as a function of pH, the core
654 rich in triacylglycerols was stained with nile red (red colour) and the proteins located at the surface of
655 the oil bodies were stained with fast green FCF (green colour) fluorescent dyes. The scale bars
656 correspond to 10 µm. The arrows indicate coalescence of OBs at the periphery of OB aggregates.
657
658 **Figure 7:** Impact of sodium chloride (NaCl) on hemp seed oil bodies (OBs) dispersions obtained by
659 aqueous extraction. **(A)** Zeta-potential of OBs as a function of NaCl concentration. **(B)** physical
660 stability of OB dispersions as a function of NaCl concentration as indicated in the figure. **(C)** Confocal
661 laser scanning microscopy images of OB dispersions in presence of various amounts of NaCl as
662 indicated in the figure (samples from figure B); the hydrophobic lipid core of OBs was stained with

663 Nile red fluorescent dye (red colour) and the proteins were stained with fast green FCF fluorescent
664 dye (green colour). Scale bars correspond to 10 µm.

665

666 **Figure 8:** Impact of calcium chloride ($CaCl_2$) on hemp seed oil bodies (OBs) dispersions obtained by
667 aqueous extraction. **(A)** Zeta-potential of OBs as a function of $CaCl_2$ concentration. **(B)** physical
668 stability of OB dispersions as a function of $CaCl_2$ concentration as indicated in the figure. **(C)** Confocal
669 laser scanning microscopy images of OB dispersions in presence of various amounts of $CaCl_2$ as
670 indicated in the figure (samples from figure B); the hydrophobic lipid core of OBs was stained with
671 Nile red fluorescent dye (red colour) and the proteins were stained with fast green FCF fluorescent
672 dye (green colour). Scale bars correspond to 10 µm.

673

FIGURES

Figure 1

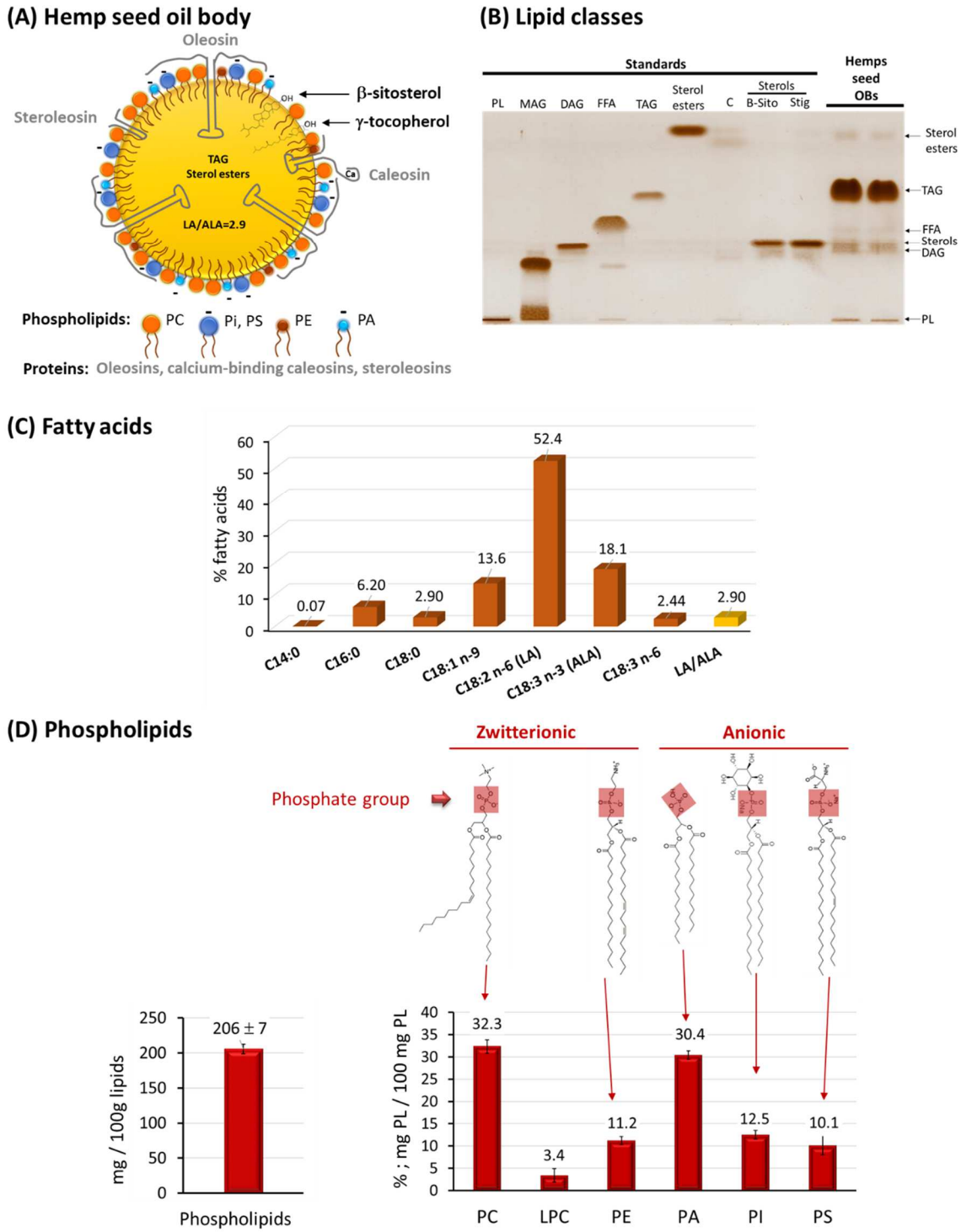

679

680 **Figure 2**

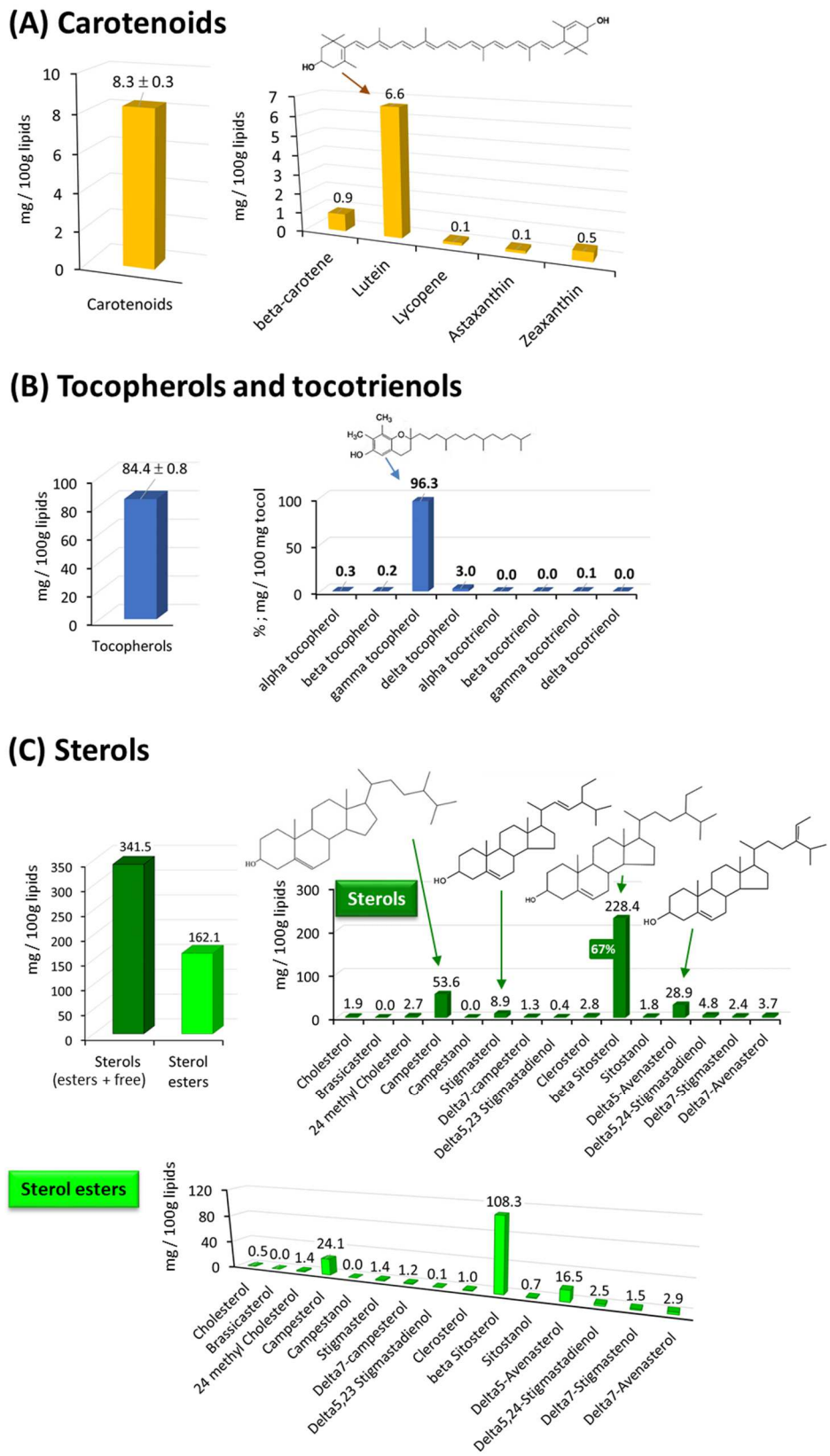

681

682 **Figure 3**

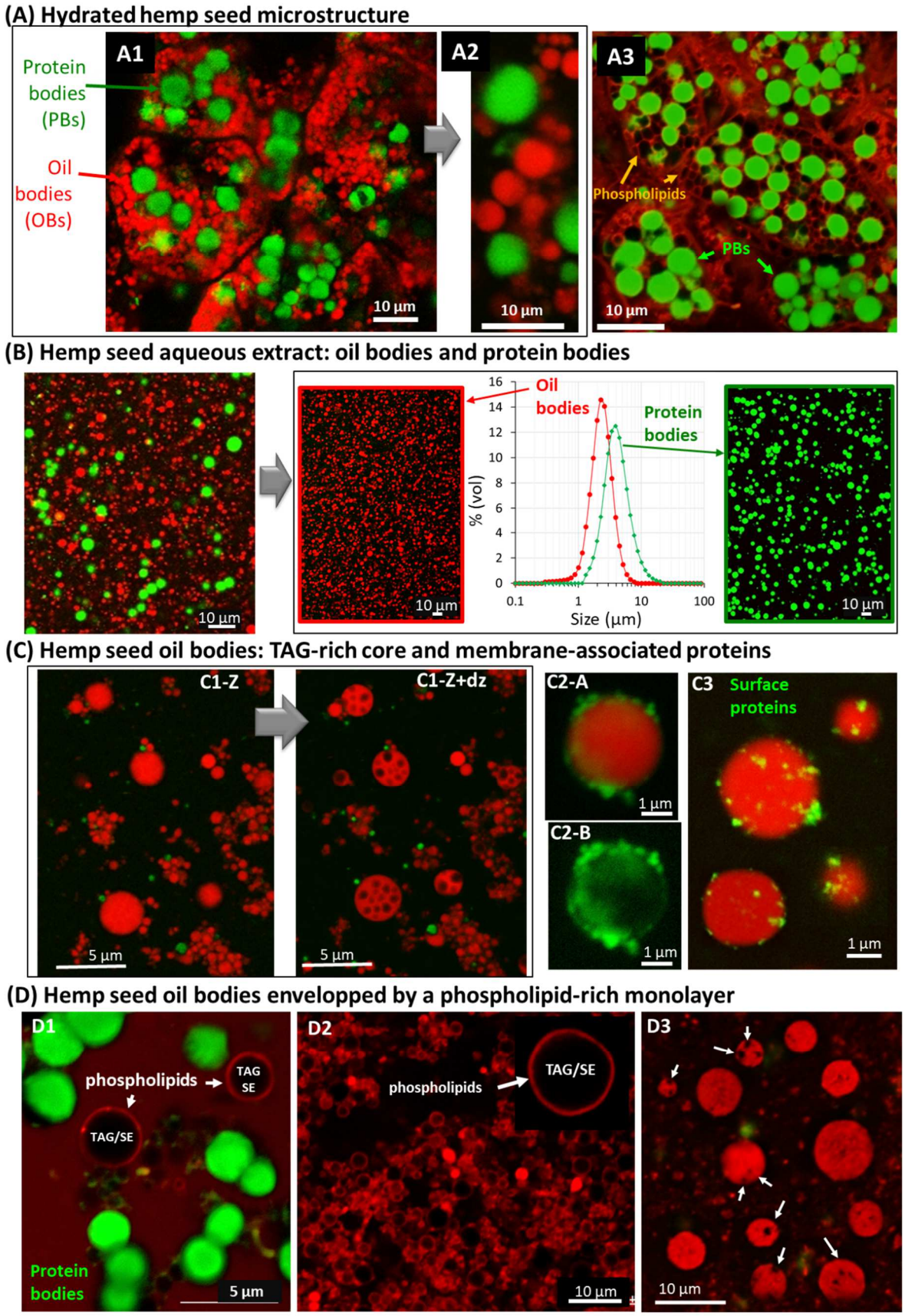

683

684 **Figure 4**

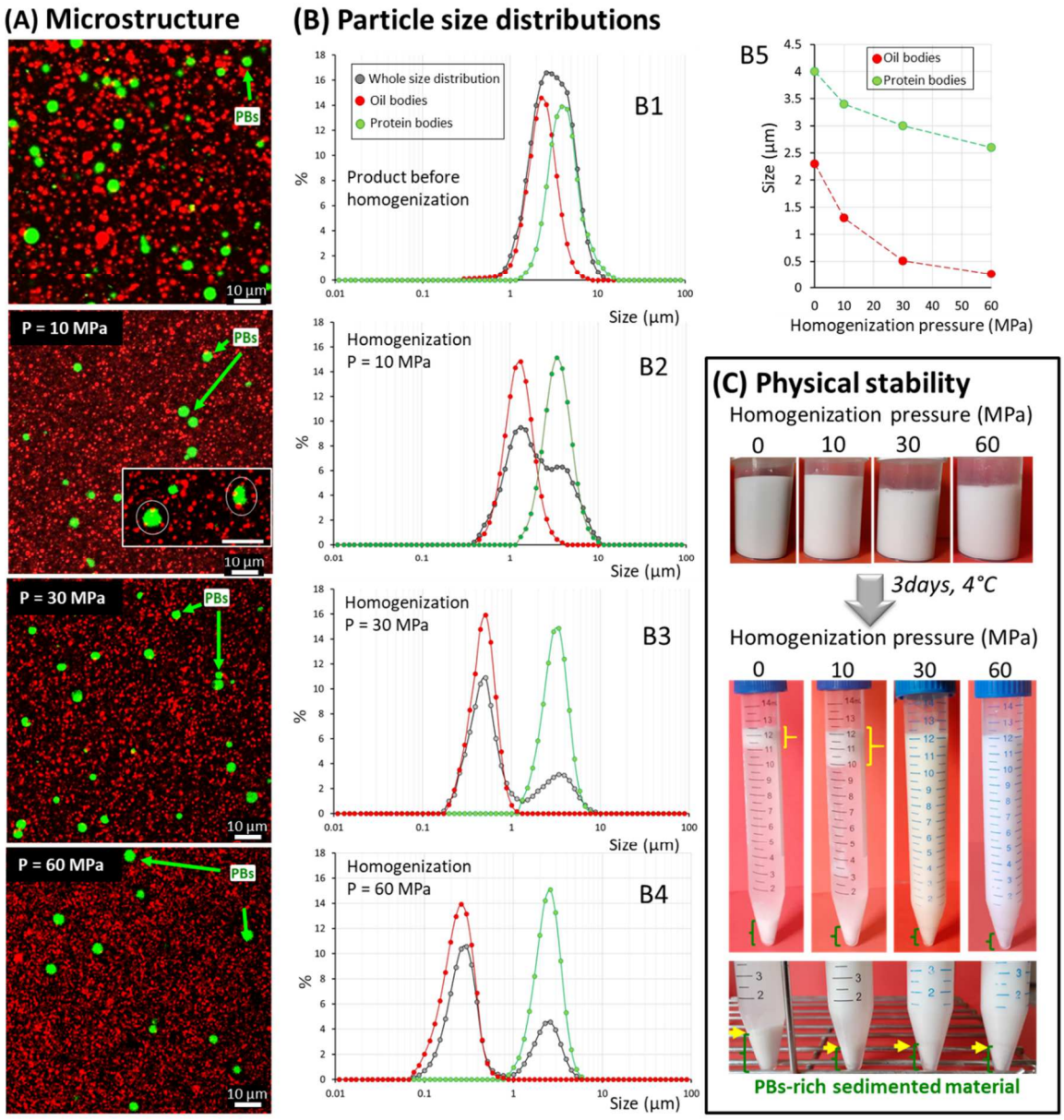

685

686

687

688

689 **Figure 5**

690

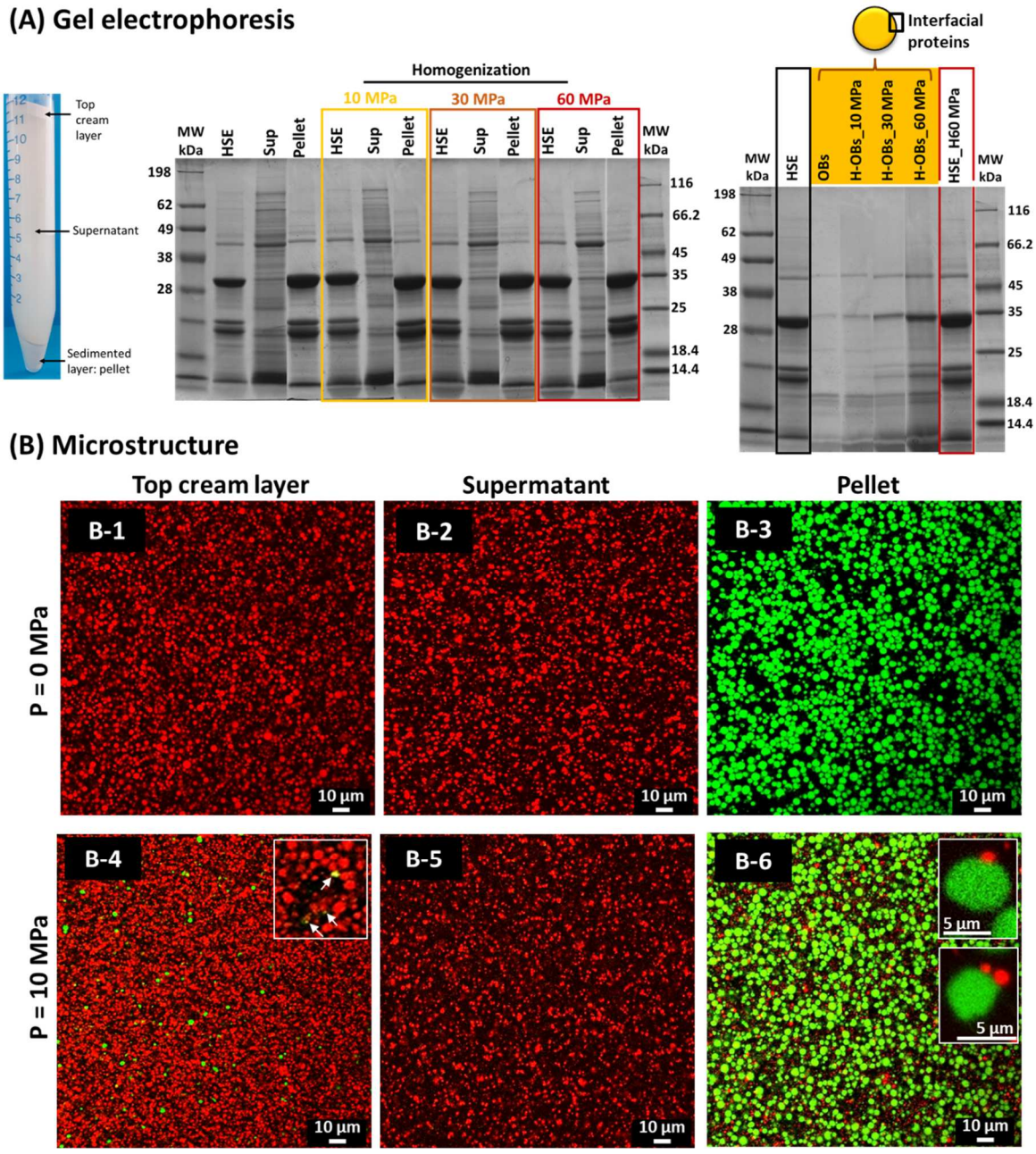

691

692

693

694 **Figure 6**

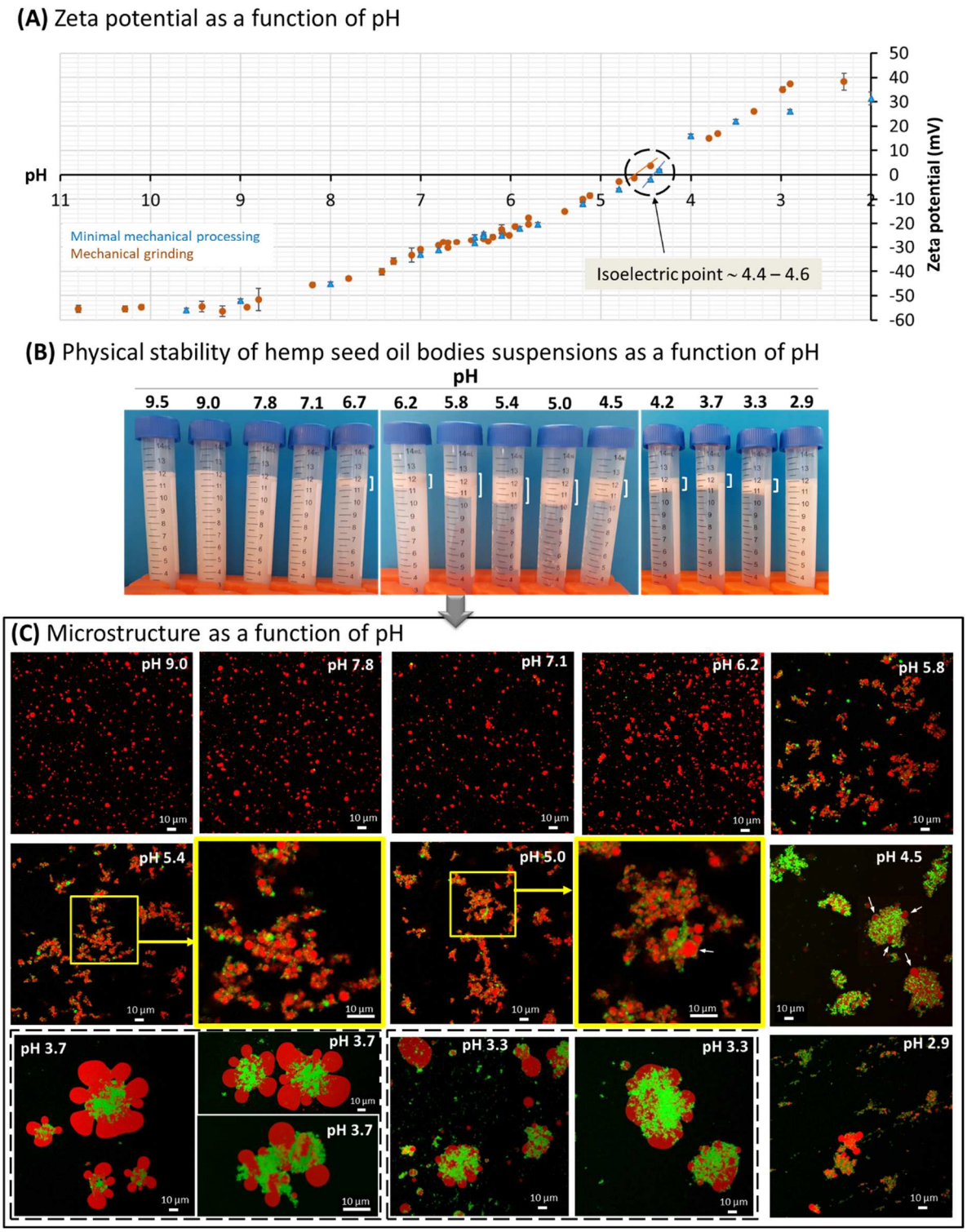

695

696

697

698 **Figure 7**

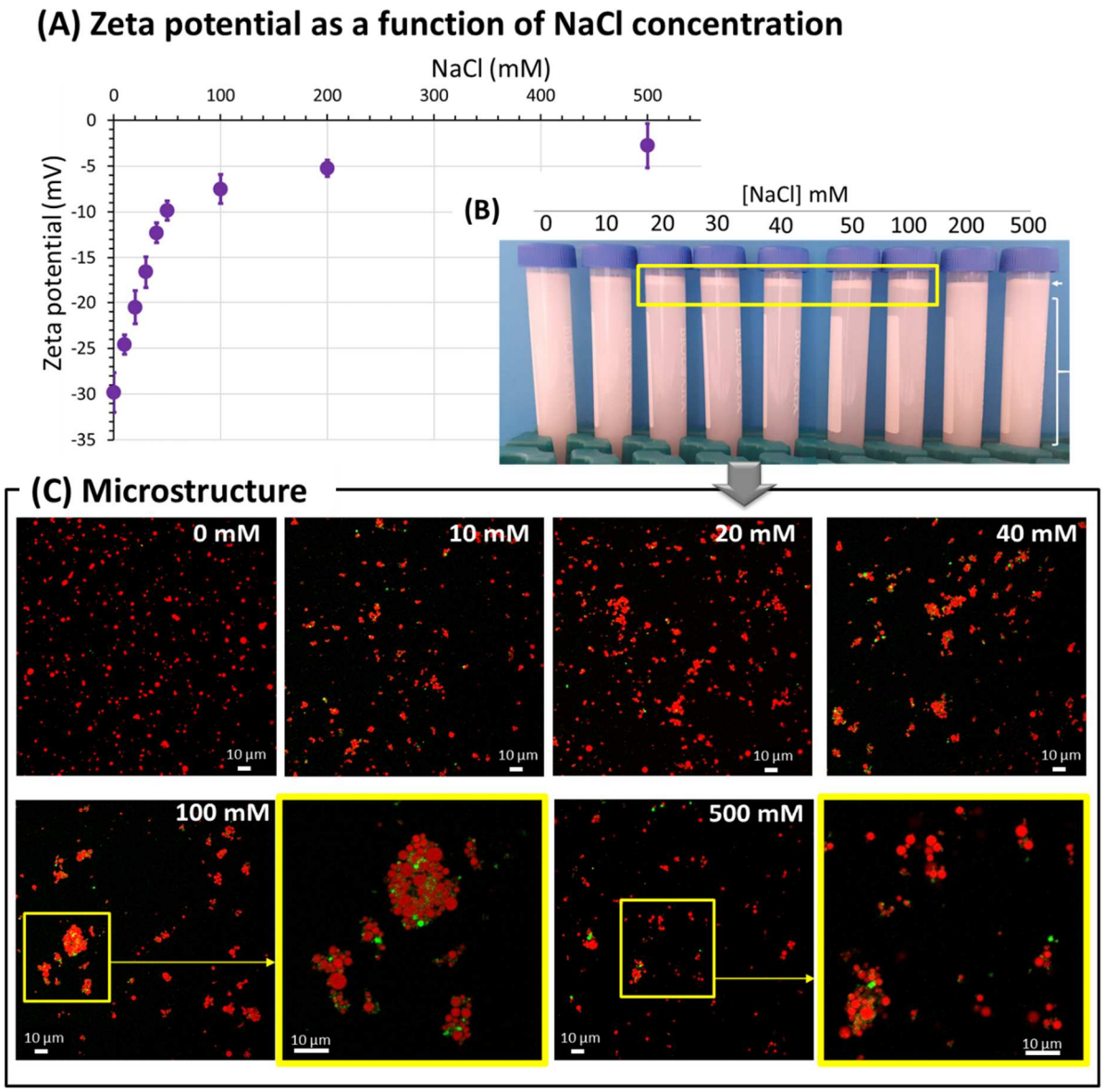

699

700

701

702

703 **Figure 8**

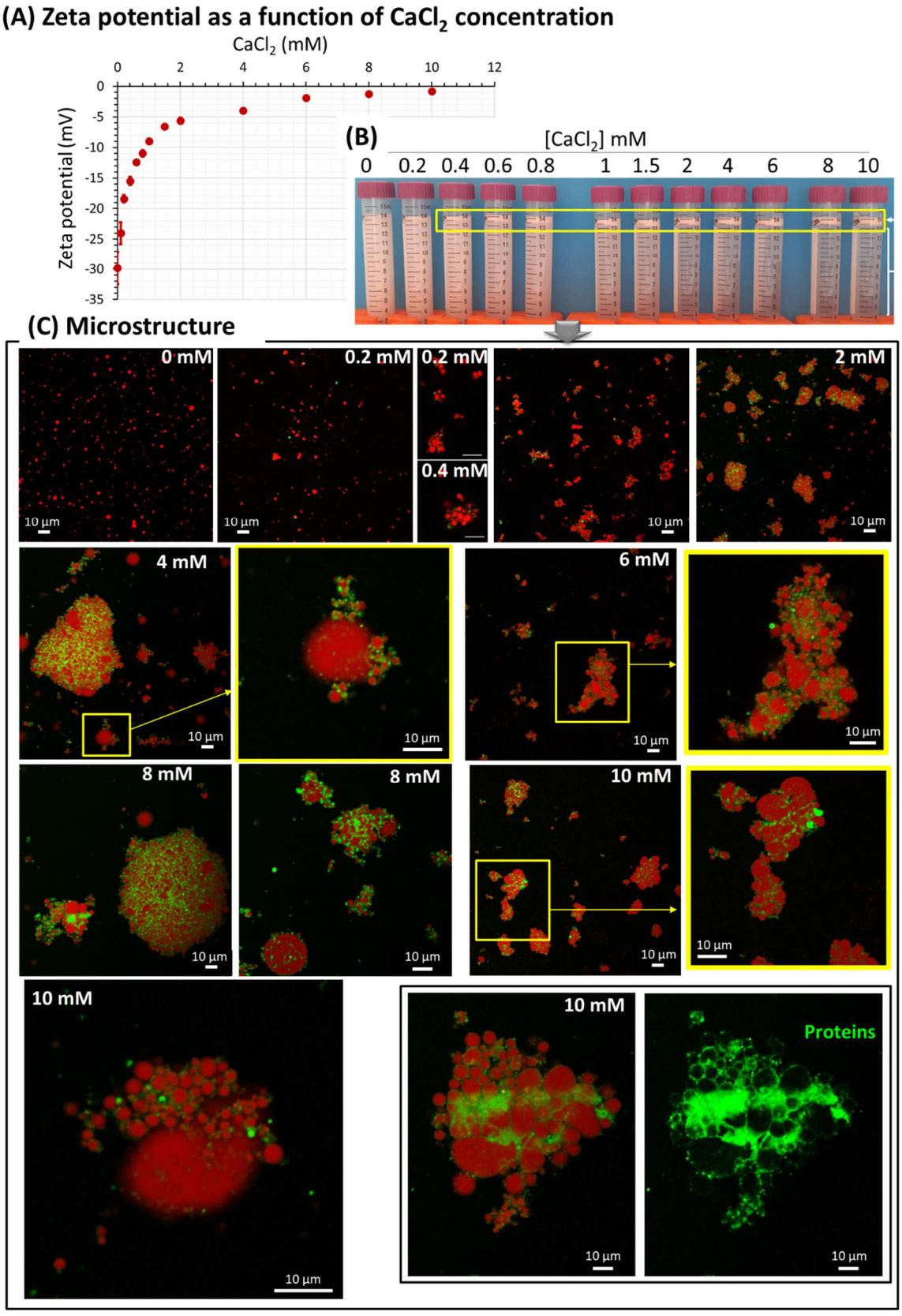

704

705

Reference list

Acevedo-Fani, A., Dave, A., Singh, H., 2020. Nature-Assembled Structures for Delivery of Bioactive Compounds and Their Potential in Functional Foods. Front Chem 8, 564021. https://doi.org/10.3389/fchem.2020.564021

Antonelli, M., Benedetti, B., Cannazza, G., Cerrato, A., Citti, C., Montone, C.M., Piovesana, S., Laganà, A., 2020. New insights in hemp chemical composition: a comprehensive polar lipidome characterization by combining solid phase enrichment, high-resolution mass spectrometry, and cheminformatics. Anal Bioanal Chem 412, 413–423. https://doi.org/10.1007/s00216-019-02247-6

Battacchi, D., Verkerk, R., Pellegrini, N., Fogliano, V., Steenbekkers, B., 2020. The state of the art of food ingredients' naturalness evaluation: A review of proposed approaches and their relation with consumer trends. Trends in Food Science & Technology 106, 434–444. https://doi.org/10.1016/j.tifs.2020.10.013

Czabany, T., Wagner, A., Zweytick, D., Lohner, K., Leitner, E., Ingolic, E., Daum, G., 2008. Structural and biochemical properties of lipid particles from the yeast Saccharomyces cerevisiae. J Biol Chem 283, 17065–17074. https://doi.org/10.1074/jbc.M800401200

Dave, A.C., Ye, A., Singh, H., 2019. Structural and interfacial characteristics of oil bodies in coconuts (Cocos nucifera L.). Food Chemistry 276, 129–139. https://doi.org/10.1016/j.foodchem.2018.09.125

Farinon, B., Molinari, R., Costantini, L., Merendino, N., 2020. The Seed of Industrial Hemp (Cannabis sativa L.): Nutritional Quality and Potential Functionality for Human Health and Nutrition. Nutrients 12, 1935. https://doi.org/10.3390/nu12071935

Folch, J., Lees, M., Stanley, G.H.S., 1957. A Simple Method for the Isolation and Purification of Total Lipides from Animal Tissues. J. Biol. Chem. 226, 497–509.

Furse, S., Liddell, S., Ortori, C.A., Williams, H., Neylon, D.C., Scott, D.J., Barrett, D.A., Gray, D.A., 2013. The lipidome and proteome of oil bodies from Helianthus annuus (common sunflower). J Chem Biol 6, 63–76. https://doi.org/10.1007/s12154-012-0090-1

Gallier, S., Gordon, K.C., Singh, H., 2012. Chemical and structural characterisation of almond oil bodies and bovine milk fat globules. Food Chemistry 132, 1996–2006. https://doi.org/10.1016/j.foodchem.2011.12.038

Huang, A.H.C., 1994. Structure of plant seed oil bodies. Current Opinion in Structural Biology 4, 493–498. https://doi.org/10.1016/S0959-440X(94)90210-0

ISO 9936:2016, n.d. Corps gras d'origines animale et végétale — Détermination des teneurs en tocophérols et en tocotriénols par chromatographie en phase liquide à haute performance [WWW Document]. ISO. URL https://www.iso.org/cms/render/live/fr/sites/isoorg/contents/data/standard/06/95/69595.html (accessed 4.27.21).

ISO-8420, 2002. Animal and vegetable fats and oils — Determination of content of polar compounds [WWW Document]. ISO. URL https://www.iso.org/cms/render/live/en/sites/isoorg/contents/data/standard/03/32/33289.html (accessed 5.21.21).

ISO-122228-1, 2014. Determination of individual and total sterols contents — Gas chromatographic method — Part 1: Animal and vegetable fats and oils [WWW Document]. ISO. URL https://www.iso.org/cms/render/live/en/sites/isoorg/contents/data/standard/06/02/60248.html (accessed 5.21.21).

Israelachvili, J., 2011. Intermolecular and Surface Forces - 3rd Edition. Elsevier.

Kapchie, V.N., Yao, L., Hauck, C.C., Wang, T., Murphy, P.A., 2013. Oxidative stability of soybean oil in oleosomes as affected by pH and iron. Food Chem 141, 2286–2293. https://doi.org/10.1016/j.foodchem.2013.05.018

755 Laemmli, U.K., 1970. Cleavage of Structural Proteins during the Assembly of the Head of
756 Bacteriophage T4. Nature 227, 680–685. https://doi.org/10.1038/227680a0
757 Lawrence, A.-M., Besir, H., 2009. Staining of Proteins in Gels with Coomassie G-250 without Organic
758 Solvent and Acetic Acid. J Vis Exp 1350. https://doi.org/10.3791/1350
759 Lopez, C., Briard-Bion, V., Ménard, O., 2014. Polar lipids, sphingomyelin and long-chain unsaturated
760 fatty acids from the milk fat globule membrane are increased in milks produced by cows fed
761 fresh pasture based diet during spring. Food Research International 58, 59–68.
762 https://doi.org/10.1016/j.foodres.2014.01.049
763 Malomo, S.A., He, R., Aluko, R.E., 2014. Structural and functional properties of hemp seed protein
764 products. J Food Sci 79, C1512-1521. https://doi.org/10.1111/1750-3841.12537
765 Marsh, D., 2013. Handbook of Lipid Bilayers, $ {number}nd édition. ed. CRC Press, Boca Raton, FL.
766 Maurer, S., Waschatko, G., Schach, D., Zielbauer, B.I., Dahl, J., Weidner, T., Bonn, M., Vilgis, T.A.,
767 2013. The role of intact oleosin for stabilization and function of oleosomes. J Phys Chem B
768 117, 13872–13883. https://doi.org/10.1021/jp403893n
769 Melcrová, A., Pokorna, S., Pullanchery, S., Kohagen, M., Jurkiewicz, P., Hof, M., Jungwirth, P., Cremer,
770 P.S., Cwiklik, L., 2016. The complex nature of calcium cation interactions with phospholipid
771 bilayers. Scientific Reports 6, 38035. https://doi.org/10.1038/srep38035
772 Montserrat-de la Paz, S., Marín-Aguilar, F., García-Giménez, M.D., Fernández-Arche, M.A., 2014.
773 Hemp (Cannabis sativa L.) seed oil: analytical and phytochemical characterization of the
774 unsaponifiable fraction. J Agric Food Chem 62, 1105–1110.
775 https://doi.org/10.1021/jf404278q
776 Naested, H., Frandsen, G.I., Jauh, G.Y., Hernandez-Pinzon, I., Nielsen, H.B., Murphy, D.J., Rogers, J.C.,
777 Mundy, J., 2000. Caleosins: Ca2+-binding proteins associated with lipid bodies. Plant Mol Biol
778 44, 463–476. https://doi.org/10.1023/a:1026564411918
779 NF-EN-12823-2, 2001. Foodstuffs - Determination of vitamin A by high performance liquid
780 chromatography - Part 2 : measurement of beta-carotene, NF EN 12823-2 - January 2001
781 [WWW Document]. URL https://m.boutique.afnor.org/standard/nf-en-12823-2/foodstuffs-
782 determination-of-vitamin-a-by-high-performance-liquid-chromatography-part-2-
783 measurement-of-beta-carotene/article/668832/fa045722 (accessed 5.27.21).
784 Nikiforidis, C.V., Kiosseoglou, V., 2009. Aqueous Extraction of Oil Bodies from Maize Germ (Zea mays)
785 and Characterization of the Resulting Natural Oil-in-Water Emulsion. J. Agric. Food Chem. 57,
786 5591–5596. https://doi.org/10.1021/jf900771v
787 Nikiforidis, C.V., Matsakidou, A., Kiosseoglou, V., 2014. Composition, properties and potential food
788 applications of natural emulsions and cream materials based on oil bodies. RSC Advances 4,
789 25067–25078. https://doi.org/10.1039/C4RA00903G
790 Ntone, E., Bitter, J.H., Nikiforidis, C.V., 2020. Not sequentially but simultaneously: Facile extraction of
791 proteins and oleosomes from oilseeds. Food Hydrocolloids 102, 105598.
792 https://doi.org/10.1016/j.foodhyd.2019.105598
793 Patton, S., Huston, G.E., 1986. A method for isolation of milk fat globules. Lipids 21, 170–174.
794 https://doi.org/10.1007/BF02534441
795 Potin, F., Saurel, R., 2020. Hemp Seed as a Source of Food Proteins, in: Crini, G., Lichtfouse, E. (Eds.),
796 Sustainable Agriculture Reviews 42: Hemp Production and Applications, Sustainable
797 Agriculture Reviews. Springer International Publishing, Cham, pp. 265–294.
798 https://doi.org/10.1007/978-3-030-41384-2_9
799 Purkrtova, Z., Le Bon, C., Kralova, B., Ropers, M.-H., Anton, M., Chardot, T., 2008. Caleosin of
800 Arabidopsis thaliana: Effect of Calcium on Functional and Structural Properties. J. Agric. Food
801 Chem. 56, 11217–11224. https://doi.org/10.1021/jf802305b
802 Qi, B., Ding, J., Wang, Z., Li, Y., Ma, C., Chen, F., Sui, X., Jiang, L., 2017. Deciphering the characteristics
803 of soybean oleosome-associated protein in maintaining the stability of oleosomes as affected
804 by pH. Food Research International 100, 551–557.
805 https://doi.org/10.1016/j.foodres.2017.07.053

Román, S., Sánchez-Siles, L.M., Siegrist, M., 2017. The importance of food naturalness for consumers: Results of a systematic review. Trends in Food Science & Technology 67, 44–57. https://doi.org/10.1016/j.tifs.2017.06.010

Romero-Guzmán, M.J., Köllmann, N., Zhang, L., Boom, R.M., Nikiforidis, C.V., 2020. Controlled oleosome extraction to produce a plant-based mayonnaise-like emulsion using solely rapeseed seeds. LWT 123, 109120. https://doi.org/10.1016/j.lwt.2020.109120

Rupasinghe, H.P.V., Davis, A., Kumar, S.K., Murray, B., Zheljazkov, V.D., 2020. Industrial Hemp (Cannabis sativa subsp. sativa) as an Emerging Source for Value-Added Functional Food Ingredients and Nutraceuticals. Molecules 25. https://doi.org/10.3390/molecules25184078

Sarkar, A., Dickinson, E., 2020. Sustainable food-grade Pickering emulsions stabilized by plant-based particles. Current Opinion in Colloid & Interface Science, Emulsions and Microemulsions 49, 69–81. https://doi.org/10.1016/j.cocis.2020.04.004

Simopoulos, A.P., 2002. The importance of the ratio of omega-6/omega-3 essential fatty acids. Biomed Pharmacother 56, 365–379. https://doi.org/10.1016/s0753-3322(02)00253-6

Smith, P.K., Krohn, R.I., Hermanson, G.T., Mallia, A.K., Gartner, F.H., Provenzano, M.D., Fujimoto, E.K., Goeke, N.M., Olson, B.J., Klenk, D.C., 1985. Measurement of protein using bicinchoninic acid. Analytical Biochemistry 150, 76–85. https://doi.org/10.1016/0003-2697(85)90442-7

Sorrentino, G., 2021. Introduction to emerging industrial applications of cannabis (Cannabis sativa L.). Rend Lincei Sci Fis Nat 1–11. https://doi.org/10.1007/s12210-021-00979-1

St Angelo, A.J., Yatsu, L.Y., Altschul, A.M., 1968. Isolation of edestin from aleurone grains of Cannabis sativa. Arch Biochem Biophys 124, 199–205. https://doi.org/10.1016/0003-9861(68)90320-2

Tang, C.-H., Ten, Z., Wang, X.-S., Yang, X.-Q., 2006. Physicochemical and Functional Properties of Hemp (Cannabis sativa L.) Protein Isolate. J. Agric. Food Chem. 54, 8945–8950. https://doi.org/10.1021/jf0619176

Tully, R.E., Beevers, H., 1976. Protein Bodies of Castor Bean Endosperm: Isolation, Fractionation, and the Characterization of Protein Components. Plant Physiology 58, 710–716. https://doi.org/10.1104/pp.58.6.710

Tzen, J., Cao, Y., Laurent, P., Ratnayake, C., Huang, A., 1993. Lipids, Proteins, and Structure of Seed Oil Bodies from Diverse Species. Plant Physiol 101, 267–276.

Tzen, J., Huang, A.H.C., 1992. Surface structure and properties of plant seed oil bodies. J Cell Biol 117, 327–335. https://doi.org/10.1083/jcb.117.2.327

Tzen, J.T., Lie, G.C., Huang, A.H., 1992. Characterization of the charged components and their topology on the surface of plant seed oil bodies. Journal of Biological Chemistry 267, 15626–15634. https://doi.org/10.1016/S0021-9258(19)49582-3

Wang, W., Cui, C., Wang, Q., Sun, C., Jiang, L., Hou, J., 2019. Effect of pH on physicochemical properties of oil bodies from different oil crops. J Food Sci Technol 56, 49–58. https://doi.org/10.1007/s13197-018-3453-y

White, D.A., Fisk, I.D., Mitchell, J.R., Wolf, B., Hill, S.E., Gray, D.A., 2008. Sunflower-seed oil body emulsions: Rheology and stability assessment of a natural emulsion. Food Hydrocolloids 22, 1224–1232. https://doi.org/10.1016/j.foodhyd.2007.07.004

Wilschut, J., Duezguenes, N., Papahadjopoulos, D., 1981. Calcium/magnesium specificity in membrane fusion: kinetics of aggregation and fusion of phosphatidylserine vesicles and the role of bilayer curvature. Biochemistry 20, 3126–3133. https://doi.org/10.1021/bi00514a022

Yang, N., Su, C., Zhang, Y., Jia, J., Leheny, R.L., Nishinari, K., Fang, Y., Phillips, G.O., 2020. In situ nanomechanical properties of natural oil bodies studied using atomic force microscopy. Journal of Colloid and Interface Science 570, 362–374. https://doi.org/10.1016/j.jcis.2020.03.011

Zaaboul, F., Raza, H., Chen, C., Liu, Y., 2018. Characterization of Peanut Oil Bodies Integral Proteins, Lipids, and Their Associated Phytochemicals. Journal of Food Science 83, 93–100. https://doi.org/10.1111/1750-3841.13995

857

858

Lopez et al.

Graphical abstract